

Downregulated Trophinin-Associated Protein Plays a Critical Role in Human Hepatocellular Carcinoma Through Upregulation of Tumor Cell Growth and Migration

Yifan Lian,^{*1} Weiming Fan,^{†1} Yanlin Huang,[‡] Hongbo Wang,^{*} Jiali Wang,^{*} Liang Zhou,[‡] Xiaojuan Wu,[‡] Meihai Deng,[†] and Yuehua Huang^{*‡}

^{*}Guangdong Province Key Laboratory of Liver Disease Research, The Third Affiliated Hospital of Sun Yat-Sen University, Guangzhou, P.R. China

[†]Department of Hepatobiliary Surgery, The Third Affiliated Hospital of Sun Yat-Sen University, Guangzhou, P.R. China

[‡]Department of Infectious Diseases, The Third Affiliated Hospital of Sun Yat-Sen University, Guangzhou, P.R. China

Trophinin-associated protein (TROAP) was a protein first identified to mediate the process of embryo transplantation and later found to be involved in microtubule regulation. However, little is known about the role of TROAP in hepatocellular carcinoma (HCC). In the present study, we reported that both TROAP mRNA and protein expressions were downregulated in human HCC samples as well as cell lines. A high level of TROAP was associated with small tumor size ($p < 0.05$), minor tumor nodules ($p < 0.01$), and mild vein invasion ($p < 0.05$). We further constructed in vitro TROAP depletion and overexpression HCC cell models. TROAP depletion significantly enhanced the proliferation and colony formation abilities, whereas TROAP overexpression had an inhibitory effect on the growth of HCC cells. The G₁/S phase arrest by TROAP overexpression correlated with increased cell cycle inhibitors p21 and p27, and declined cell cycle promoting kinase complex CDK6/cyclin D1. Depressed TROAP expression enhanced the migration ability, while the opposite influence was observed in TROAP-overexpressed HCC cells. Taken together, these results indicate that TROAP suppresses cellular growth and migration in HCC. This discovery will further our understanding of the pathogenic mechanisms of human HCC.

Key words: Trophinin-associated protein (TROAP); Hepatocellular carcinoma (HCC); Cell cycle; Tumor growth; Migration

INTRODUCTION

Hepatocellular carcinoma (HCC) is the third leading cause of cancer deaths worldwide, with an estimated 500,000–600,000 deaths per year^{1,2}. HCC development is driven by the interaction of genetic predisposition, environmental factors (metabolic syndrome, alcohol, and aflatoxin B1), and virus infection³. Despite advances in the detection rate of early stage HCC patients, the 5-year overall survival rate of HCC patients, particularly in the intermediate and advanced stages, remains extremely low^{4,5}. In addition, curative treatment including liver transplantation and hepatic resection are only suitable for fewer than 20% of HCC patients, and no adequate effective therapy remains for HCC due to late stage diagnosis or,

frequently, relapse⁶. Therefore, there is a strong need to discover novel biomarkers of diagnosis, therapy, and prognosis for HCC.

Over the past decades, improvements have been made to clarify the molecular pathogenesis of HCC. Genomic analyses have allowed the identification of six major pathways that are recurrently responsible for the initiation and progression of HCC^{7,8}. Common mutations affect the telomere maintenance [telomerase reverse transcriptase (TERT)], activation of Wntless-related integration site (Wnt)/ β -catenin pathway [catenin β 1 (CTNNB1), axis inhibitor 1 (AXIN1), or adenomatous polyposis coli (APC)], suppression of tumor protein p53 (TP53) and the cell cycle pathway [cyclin-dependent kinase inhibitor 2A

¹These authors provided equal contribution to this work.

Address correspondence to Yuehua Huang, M.D., Ph.D., Department of Infectious Diseases and Guangdong Provincial Key Laboratory of Liver Disease Research, The Third Affiliated Hospital of Sun Yat-Sen University, 600 Tian He Road, Guangzhou 510630, P.R. China. Tel: 8620-85252702; Fax: 8620-85253305; E-mail: huangyh53@mail.sysu.edu.cn or Meihai Deng, M.D., Department of Hepatobiliary Surgery, The Third Affiliated Hospital of Sun Yat-Sen University, 600 Tian He Road, Guangzhou 510630, P.R. China. Tel: 8620-85252700; Fax: 8620-85253305; E-mail: drdmh@medmail.com.cn

(CDKN2A) or retinoblastoma 1 (RB1)], overload of oxidative stress [nuclear factor erythroid 2-related factor 2 (NRF2) or kelch-like erythroid cell-derived protein with cap 'n' collar (CNC) homology (ECH)-associated protein 1 (KEAP1)], alteration of epigenome modifiers [adenine–thymine (AT)-rich interaction domain 1A (ARID1A) or ARID2], and activation of the RAS/mitogen-activated protein kinase (RAS/MAPK) pathway. Spindle assembly has long been known to participate in the regulation of the cell cycle⁹. During mitosis, chromosome segregation is mediated by a complex microtubule (MT)-based structure, the spindle. The proper assembly and function of the mitotic spindle are essential for the equal distribution of genetic material to two daughter cells, and errors in this process result in genomic instability, generating aneuploid or polyploid cells^{10,11}. Such genomic imbalances are among the most common characteristics of cancer and are considered to be crucial for tumorigenesis.

Trophinin-associated protein (TROAP), formally known as tasin, was first identified as a protein that forms a complex with trophinin and bystin at the uteroplacental interface of the trophoblasts and endometrium by Fukuda and colleagues¹². This complex functions in early embryo implantation, which is accompanied by rapid cellular invasion and proliferation^{13–15}. Previous studies have indicated that TROAP mRNA presents a spatial expression profile, with high levels in the testis, bone marrow, and thymus^{16,17}. TROAP's function was only implicated in embryo implantation until several studies revealed that TROAP could be an MT-associated protein and regulate the proper spindle assembly during mitosis. TROAP is primarily localized on the MTs, centrosomes, and the mitotic spindle during the cell cycle. Overexpression of TROAP led to monopolar spindle formation, whereas loss of TROAP expression caused mitotic block and induced multipolar spindles, indicating its importance in proper spindle assembly. Interestingly, TROAP is highly expressed in human cancer cell lines such as HeLa and Jurkat cells^{18,19}. However, little is known about TROAP's role in cancer development.

In the present study, we showed that TROAP is downregulated in HCC tissues and cell lines, and its expression level is correlated with tumor size, nodule number, and vein invasion status. Using small interfering RNA (siRNA) depletion and overexpression HCC cell models, we demonstrated that TROAP inhibits cell proliferation and clonogenic and migration abilities through induction of the G₁/S phase arrest. Overexpression of TROAP also leads to upregulation of the cycle-dependent kinase inhibitors 1A (p21) and 1B (p27) and downregulation of the cyclin-dependent kinase 6 (CDK6)/cyclin D1 complex. These results suggest a significant role of TROAP in tumor growth and metastasis of human HCC.

MATERIALS AND METHODS

Antibodies

Commercially available antibodies were as follows: TROAP (NBP1-92532; Novus Biologicals, Littleton, CO, USA), glyceraldehyde 3-phosphate dehydrogenase (GAPDH; 60004-1-Ig; Proteintech, Chicago, IL, USA), cyclin D1 (2978; Cell Signaling Technology, Danvers, MA, USA), CDK6 (13331; Cell Signaling Technology), p21 (2947; Cell Signaling Technology), and p27 (3686; Cell Signaling Technology).

Cell Lines

The immortalized hepatic cell line LO2 and seven human liver cancer cell lines 97L, HepG2, Hep3B, Huh7, SMMC-7721, BEL7404, and QGY-7703 were obtained from the Third Affiliated Hospital of Sun Yat-Sen University (Guangzhou, P.R. China). All cell lines were thawed from early passage stocks, passaged for less than 6 months, and cultured in Dulbecco's modified Eagle's medium (DMEM; Life Technologies, Grand Island, NY, USA) supplemented with 10% fetal bovine serum (FBS; Gibco, Grand Island, NY, USA). Cells were grown in a humidified 5% CO₂ incubator at 37°C and passaged using standard cell culture techniques.

Reverse Transcription Polymerase Chain Reaction (RT-PCR)

Total RNA was extracted from HCC tissues and cells using TRIzol Reagent (Invitrogen, Grand Island, NY, USA) following the manufacturer's instructions. Subsequently, a total of 2 µg of purified RNA from each sample was reverse transcribed using GoScript™ Reverse Transcription System (Promega, Madison, WI, USA). Real-time quantitative RT (qRT)-PCR was performed with Platinum SYBR Green qPCR SuperMix-UDG (Invitrogen) with a LightCycler 480 PCR platform (Roche, Indianapolis, IN, USA) at the following temperature profiles: 1 cycle at 95°C (2 min), 40 cycles of denaturation at 95°C (30 s), and annealing at 60°C (1 min). Primers synthesized by Invitrogen Company (Shanghai, P.R. China) were as follows: TROAP, 5'-TG CAGAAACCACCGCTCAATA-3' (forward) and 5'-CC ACCAATCTTTGTGATGTCTCT-3' (reverse); GAPDH, 5'-GGAGCGAGATCCCTCCAAAAT-3' (forward) and 5'-GGCTGTTGTCATACTTCTCATGG-3' (reverse). The GAPDH mRNA was used as internal standard reference. Normalized expression was calculated using the comparative C_T method, and fold changes were derived from the 2^{-ΔΔC_T} values for each gene. The PCR experiments were done in triplicate.

Plasmids and Transfection

The full-length human TROAP cDNA was amplified from the cDNA library of QGY-7703 cells and subcloned

into a pLVX-DsRed-Monomer-N1 vector purchased from Clontech (Mountain View, CA, USA). Lentivirus produced in 293T cells was used to infect SMMC-7721 and QGY-7703 human HCC cells by spinfection ($500\times g$ for 1.5 h) and incubated overnight, followed by selection with $2\ \mu\text{g}/\text{ml}$ of puromycin (P8833; Sigma-Aldrich, St. Louis, MO, USA) for 2 weeks. Stable overexpression of TROAP was validated by Western blotting.

Two targeting TROAP siRNA duplexes (TROAP RNA#1, 5'-GTAGGATTGAGCCTGAGAT-3'; TROAP RNA#2, 5'-GGAACAGCTTGAAGTACCA-3') were obtained from RiboBio Company (Guangzhou, P.R. China) and gave consistent results. SMMC-7721 and QGY-7703 were transfected with 100 nM siRNA using Lipofectamine RNAiMAX according to the manufacturer's protocol (Invitrogen, Carlsbad, CA, USA). Seventy-two hours later, the RNA interference was confirmed using Western blotting.

Proliferation Assay

Cell proliferation rate was determined using MTT assay (M6494; Thermo Scientific, Waltham, MA, USA) according to the manufacturer's protocol. Cells were seeded in five replicates in a 96-well plate at a density of 2,000 cells per well and cultured with DMEM containing 10% FBS. For 7 days, cells were incubated with $20\ \mu\text{l}$ of 5 mg/ml MTT for 4 h at 37°C . Subsequently, $150\ \mu\text{l}$ of 100% dimethyl sulfoxide (DMSO) was added to dissolve the precipitates. Viable cells were counted every day by reading the absorbance at 490 nm with a plate reader (ELx800; BioTek, Winooski, VT, USA).

Western Blot

Cells were lysed in NETN buffer (100 mM NaCl, 1 mM EDTA, 0.5%, 20 mM Tris-HCl at pH 8.0, and Nonidet P-40) containing protease and phosphatase inhibitor cocktail (Thermo Fisher Scientific, Rockford, IL, USA). The lysate protein concentration was measured using the bicinchoninic acid (BCA) protein assay kit (Pierce, Rockford, IL, USA); after normalization to equal amounts, proteins were separated by 8% or 10% sodium dodecyl sulfate-polyacrylamide gel electrophoresis (SDS-PAGE), transferred to polyvinylidene fluoride (PVDF) membranes, and probed with the indicated primary antibodies. The blots were then incubated with species-specific horseradish peroxidase (HRP)-conjugated secondary antibodies, and the immunoreactive bands were visualized by enhanced chemiluminescence (ECL; Pierce).

Colony Formation Assay

Cells were seeded into six-well plates at a density of 2,000 per well and incubated at 37°C and at an atmosphere of 5% CO_2 for 14 days. Additional culture medium was added to the plates at day 3. Cells were fixed with

methanol, stained with 0.5% crystal violet (C6158; Sigma-Aldrich), and dried. Only clearly visible colonies (more than 50 cells) were counted under a light microscope. The test was repeated three times.

Transwell Assay

Cells were trypsinized and pelleted by centrifugation. After washing twice in phosphate-buffered saline (PBS), the cells were resuspended in serum-free DMEM at a density of 8×10^5 cells/ml, and $200\ \mu\text{l}$ of the cell suspension was seeded onto the basement Matrigel-coated membrane matrix (BD Biosciences, San Jose, CA, USA). FBS was added to the lower chamber as a chemoattractant. After 20 h, the noninvading cells were gently removed with a cotton swab. Invasive cells located on the lower side of the chamber were fixed with 4% paraformaldehyde (PFA; Sigma-Aldrich) for 20 min at room temperature prior to crystal violet staining. Three independent visual fields were examined via microscopic observation, and the number of cells was determined.

Flow Cytometry

For cell cycle analysis, samples were harvested, washed twice in PBS, and then fixed in ice-cold 70% ethanol at -20°C overnight. Fixed cells were treated with RNase A (R4875; Sigma-Aldrich) for 30 min at room temperature before the addition of $5\ \mu\text{l}/\text{ml}$ propidium iodide (PI; P4864; Sigma-Aldrich) for 10 min in the dark. Cell cycle distribution was determined using a Beckman-Coulter Flow Cytometry FC500 (Brea, CA, USA). All experiments were performed at least three times.

Patients and Tissue Specimens

A total of 52 HCC specimens were obtained from patients who underwent hepatectomy in the Department of Hepatobiliary Surgery at the Third Affiliated Hospital of Sun Yat-Sen University from January 2014 to December 2015. None of the patients in our study received neoadjuvant chemotherapy. These patients included 45 males and 7 females with median age of 45 years (range: 26–68). Among these patients, 52 matched fresh HCC specimens and adjacent noncancerous liver tissues were selectively used for qRT-PCR and Western blot analysis. The diagnosis for each patient was confirmed by histopathology. Clinopathological data were compared to TROAP expression to determine whether any correlations exist. Prior informed consent was obtained, and the study protocol was approved by the Ethics Committee of the Third Affiliated Hospital of Sun Yat-Sen University.

Statistical Analysis

The SPSS software version 19.0 and GraphPad Prism 5 software were used to perform the statistical analyses. Correlation of the TROAP staining intensity to

clinicopathological characteristics was measured using Pearson's chi-square or Fisher's exact test. Each experiment was performed three times in triplicate. The significance of variances between groups was determined by the *t*-test. Unless otherwise indicated, all error bars indicate standard deviation (SD). All statistical tests were two sided, and a value of $p < 0.05$ was considered statistically significant.

RESULTS

TROAP Is Downregulated in HCC Tissues and Cell Lines

To assess the role of TROAP in HCC development and progression, we first examined TROAP expression status in HCC tissues and cell lines. TROAP mRNA levels were detected in 52 HCC tissues and matched noncancerous adjacent tissues. The results demonstrated that mRNA expression of TROAP was significantly decreased in HCC tumor tissues (Fig. 1A). We also detected the protein expression levels of TROAP in 12 pairs of tumor and

noncancerous tissues. Again, we observed that TROAP expression was downregulated in all tumor tissues compared to matched noncancerous tissues (Fig. 1B). In addition, TROAP expressions in one immortalized hepatic cell line LO2 and seven liver cancer cell lines were measured. Consistent with the tissue expression pattern, noncancerous hepatic cell line LO2 showed higher levels of both TROAP mRNA and protein than all the tumor cell lines (97L, HepG2, Hep3B, Huh7, SMMC-7721, BEL-7404, and QGY-7703) (Fig. 1C and D). These results indicated that TROAP is downregulated in HCC tissues and cell lines, suggesting a possible role in HCC development.

Decreased TROAP Expression Correlates With Poor Diagnosis in HCC Patients

To further investigate whether TROAP mRNA expression could serve as a novel diagnostic marker for HCC patients, we examined the correlations between TROAP expression with clinicopathological factors including age, gender, tumor size and number, tumor invasion, and pathological stages. The staining intensity and distribution

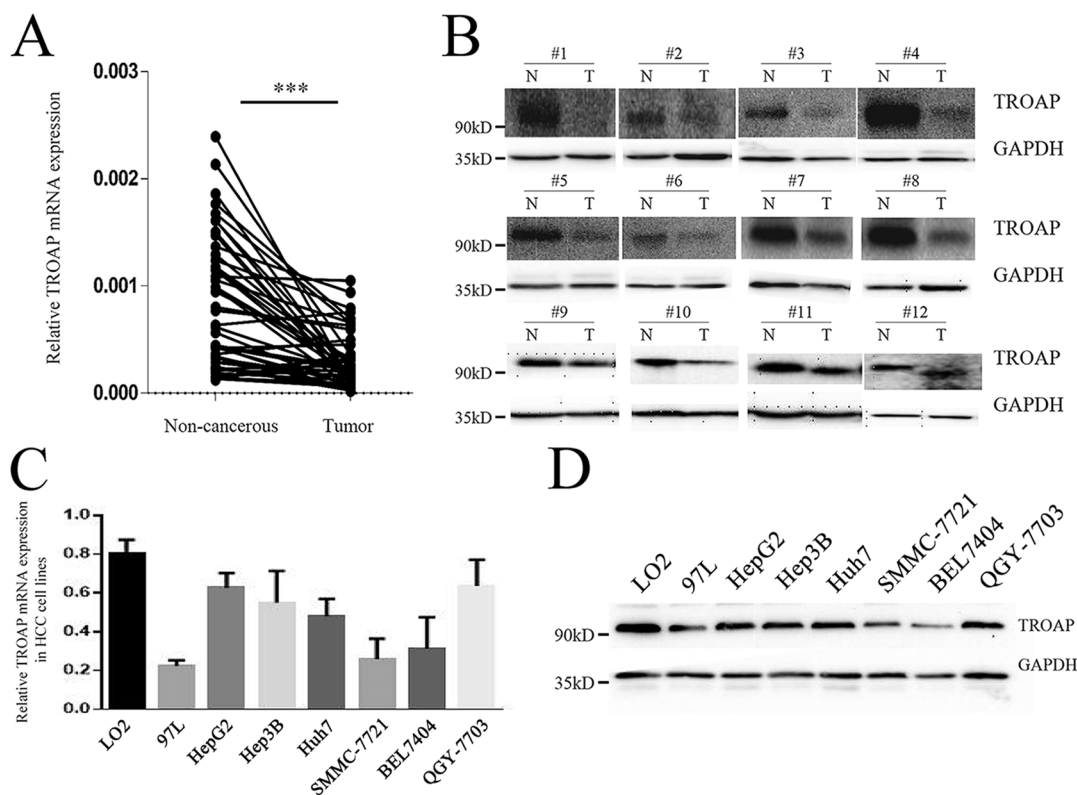


Figure 1. Trophinin-associated protein (TROAP) is downregulated in hepatocellular cancer (HCC) tissues and cell lines. (A) The mRNA levels of TROAP from 52 pairs of HCC tissues and matched noncancerous tissues were tested using quantitative reverse transcription polymerase chain reaction (qRT-PCR). *** $p < 0.001$. (B) The protein levels of TROAP in 12 pairs of HCC tissues and matched noncancerous tissues were tested by Western blotting. N, non-cancerous; T, tumor. Glyceraldehyde 3-phosphate dehydrogenase (GAPDH) was used as a loading control. The mRNA and protein expression levels of TROAP in one immortalized hepatic cell line (LO2) and seven liver cancer cell lines (97L, HepG2, Hep3B, Huh7, SMMC-7721, BEL-7404, and QGY-7703) were determined by qRT-PCR (C) and Western blotting (D), respectively. Data of qRT-PCR were presented as mean \pm standard deviation (SD).

varied among the samples, and a cutoff value according to the receiver operating characteristic (ROC) curve was used to separate patients into two groups: a low TROAP group ($n=30$) and a high TROAP group ($n=22$). As shown in Table 1, no significant correlation was found between TROAP expression and age ($p=0.9125$), gender ($p=0.9748$), α -fetoprotein (AFP) level ($p=0.7459$), cirrhosis status ($p=0.6704$; $p=0.3405$ for Child–Pugh

score), capsular formation ($p=0.3790$), and pathological stage [$p=0.3309$ for tumor–node–metastasis classification (TNM) stage; $p=0.6289$ for Edmondson–Steiner grade, except $p=0.0412$ for Barcelona clinic liver cancer (BCLC) stage]. However, we did observe that lower TROAP expression was associated significantly with larger tumor size ($p=0.0121$), multiple tumor nodules ($p=0.0035$), and presence of vein invasion ($p=0.0186$) in

Table 1. Association of TROAP mRNA Expression With Clinicopathological Parameters in 52 HCC Specimens

Clinicopathologic Variables	<i>n</i>	TROAP mRNA Expression		<i>p</i> Value
		Low	High	
Gender				0.9748
Male	45	26	19	
Female	7	4	3	
Age (years)				0.9125
≤ 60	47	27	20	
> 60	5	3	2	
AFP (ng/ml)				0.7459
< 200	13	8	5	
≥ 200	39	22	17	
Cirrhosis				0.6704
Absence	4	2	2	
Presence	48	28	20	
Child–Pugh Score				0.3405
A	34	18	16	
B	18	12	6	
Tumor size (cm)				0.0121*
< 3	35	16	19	
≥ 3	17	14	3	
Capsular formation				0.3790
Presence	3	1	2	
Absence	49	29	20	
Tumor nodule number				0.0035†
Solitary	39	18	21	
Multiple (≥ 2)	13	12	1	
TNM stage				0.3309
I–II	39	21	18	
III	13	9	4	
BCLC stage				0.0412*
0–A	32	22	10	
B–C	20	8	12	
Edmondson–Steiner				0.6289
I–II	17	9	8	
III–IV	35	21	14	
Vein invasion				0.0186*
Presence	19	15	4	
Absence	33	15	18	

AFP, α -fetoprotein; BCLC, barcelona clinic liver cancer; HCC, hepatocellular cancer; TNM, tumor–node–metastasis classification; TROAP, trophinin-associated protein.

* $p < 0.05$; † $p < 0.01$.

the detected samples. These results indicated that TROAP mRNA expression may therefore be useful for the diagnosis of tumor size, nodule number, and invasion status in HCC patients.

TROAP Has an Inhibitory Effect on HCC Cell Growth

To characterize the functional role of TROAP in HCC development, we constructed TROAP knockdown and overexpressed cell models in two HCC cell lines, QGY-7703 and SMMC-7721. As depicted in Figure 2A, TROAP protein levels were verified in both knockdown and overexpressed cells, indicating successful establishment of in vitro cell models. We then measured the effect of TROAP depletion or overexpression on HCC cell growth. We found that TROAP-depleted cells multiplied significantly faster than the control cells. On the other hand, TROAP upregulation caused suppression on tumor cell proliferation (Fig. 2B). The colony formation assay also confirmed that TROAP-depleted cells generated fewer numbers of cell colonies with a smaller size than

the control cells (Fig. 2C), while TROAP-overexpressed cells had a larger number of cell colonies after the cultivation (Fig. 2D). Taken together, these results suggested that TROAP played a tumor-suppressive role in HCC cell growth.

TROAP Overexpression Leads to G₁/S Phase Arrest on HCC Cells

Cell cycle dysregulation has been shown to be involved in tumor growth inhibition. To clarify the underlying mechanism responsible for TROAP-mediated HCC cell growth and clonogenicity inhibition, we detected the cell cycle distributions of both TROAP knockdown and overexpressed cells through flow cytometry. In the TROAP-depleted HCC cells, a nonsignificant smaller proportion of the G₁ phase cells was observed, with a nonsignificant small increase in the S phase cells and limited change in the G₂/M phase cells (Fig. 3A). We demonstrated that the proportion of G₁ phase cells increased significantly after TROAP overexpression, while there were significantly

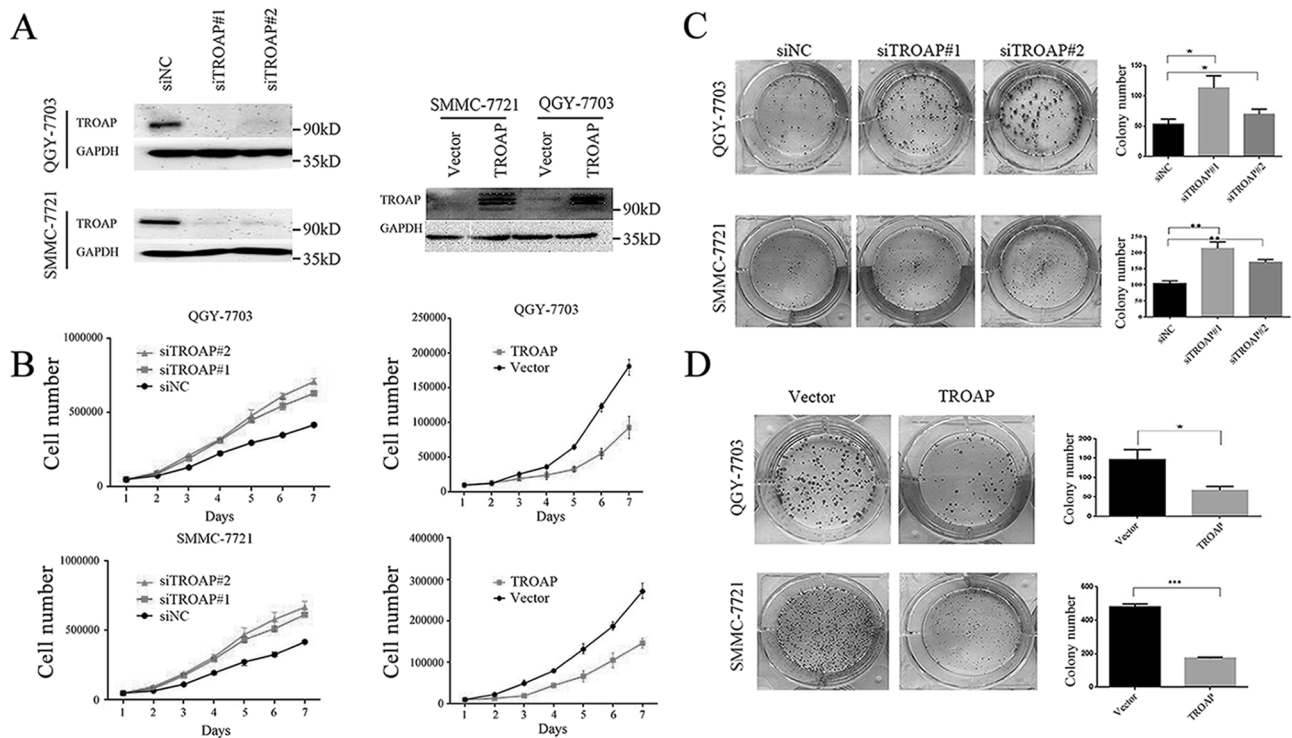


Figure 2. TROAP has an inhibitory effect on HCC cell growth. (A) The effects of TROAP knockdown with small interfering RNAs (siRNAs) 72 h after transfection (left) or plasmid TROAP overexpression (right) were verified by Western blotting in QGY-7703 and SMMC-7721 cells. (B) Cell viability of TROAP knockdown (left) or overexpression (right) was determined using MTT assay at indicated times in QGY-7703 and SMMC-7721 cells. Data were presented as mean \pm SD. (C) Colony formation assays of QGY-7703 and SMMC-7721 cells transfected with negative control (NC) and TROAP-targeted siRNAs. Left: representative images; right: quantification of the colony numbers. Data were presented as mean \pm SD. * p < 0.05, ** p < 0.01. (D) Colony formation assays of control and TROAP-overexpressed HCC cells. Left: representative images; right: quantification of the colony numbers. Data were presented as mean \pm SD. * p < 0.05, *** p < 0.001.

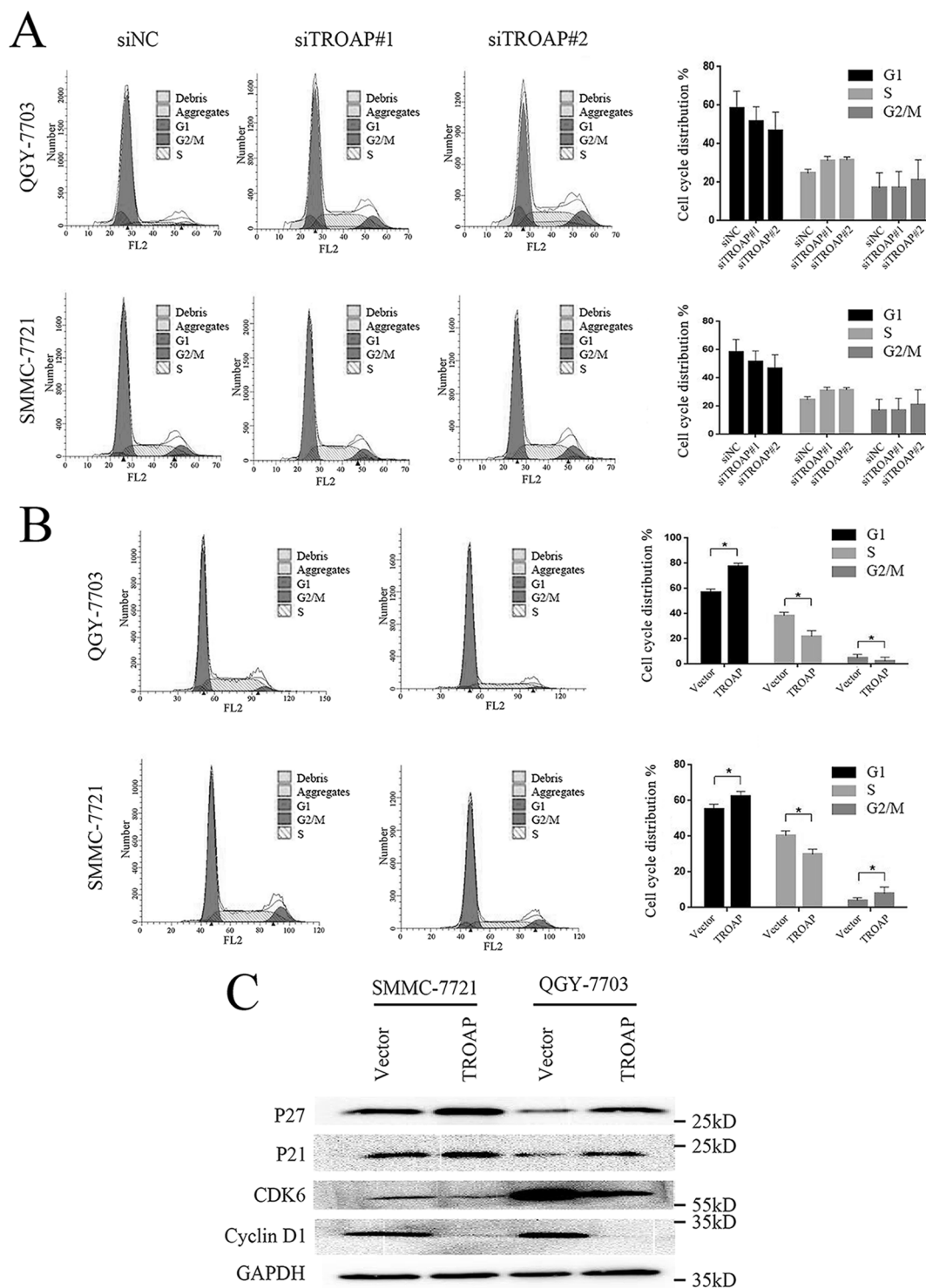


Figure 3. TROAP overexpression leads to G₁/S phase arrest on HCC cells. (A) Cell cycle distributions of QGY-7703 and SMMC-7721 cells transfected with control or TROAP siRNAs for 48 h were determined by flow cytometry. Left: representative images; right: summary of the results. Data were presented as mean±SD. (B) Cell cycle distributions of control or TROAP-overexpressed QGY-7703 and SMMC-7721 cells were determined by flow cytometry. Left: representative images; right: summary of the results. Data were presented as mean±SD. **p*<0.05. (C) Western blotting analysis of expressions of cycle-dependent kinase inhibitors 1B (p27), 1A (p21), cyclin-dependent kinase 6 (CDK6), and cyclin D1 in control or TROAP-overexpressed QGY-7703 and SMMC-7721 cells.

decreased percentages of the S and G₂/M phase cells (Fig. 3B). We further measured the expression levels of several proteins important for G₁/S phase transition in TROAP overexpression cells. Consistent with the flow cytometry data, expressions of cell cycle inhibitors p27 and p21 increased significantly, while levels of cell cycle promoting kinase complex CDK6 and cyclin D1 declined remarkably after TROAP upregulation (Fig. 3C). These results indicated that TROAP overexpression induced G₁/S phase arrest, thus causing an inhibitory effect on HCC cell growth.

TROAP Reduces the Migration Ability of HCC Cells

Aberrant cell migration is frequently associated with cancer, and enhanced migration ability is generally believed to be associated with tumor metastasis. TROAP was previously identified as an associated protein mediating the attachment of embryonic cells to the maternal epithelial cells, inducing rapid cellular invasion and proliferation. We therefore measured whether TROAP could affect the cell migration ability in HCC cell models. We found that by the Transwell assay, more TROAP-depleted cells were observed at the bottom of the wells after overnight incubation (Fig. 4A), while a smaller number of cells passed through the upper chamber in the TROAP-overexpressed cells (Fig. 4B). These data indicated that TROAP overexpression might reduce the migration ability of HCC cells.

DISCUSSION

In the present study, we demonstrated that TROAP was downregulated in HCC tissues and cell lines. The expression level of TROAP mRNA was associated with tumor size, nodule number, and vein invasion status in HCC. Using *in vitro* HCC cell models, we also showed that TROAP depletion was required for enhanced cellular proliferation, colony formation, and migration. Accordingly, TROAP plays a significant inhibitory role on tumor growth and metastasis and may be a potential diagnostic biomarker for HCC.

TROAP was reported to be highly expressed in cancer cell lines such as HeLa and Jurkat cells¹⁹. A cDNA microarray analysis has also indicated that TROAP expression is upregulated in prostate cancer tissues²⁰. Data mining of the open access online databases (The Cancer Genome Atlas, Oncomine, Human Protein Atlas) also showed that TROAP expression was higher in HCC tumor than in normal adjacent tissue. However, our data demonstrated that both mRNA and protein expressions of TROAP were decreased in HCC tissues and cell lines. The inconsistency to the above research may come from the different origins of the detection samples. Our HCC samples originated from hepatitis B virus (HBV)-infected patients, which were dominant in China. Previous studies were

performed with HCC tissues related to alcohol, hepatitis C virus (HCV), or nonalcoholic steatohepatitis (NASH). Molecular pathogenesis can be different in HCCs according to their etiology²¹⁻²³. Therefore, further investigations are required to clarify this discrepancy.

The spindle assembly checkpoint (SAC) is the major cell cycle control mechanism in mitosis. It ensures the fidelity of chromosome segregation to produce genetically identical daughter cells and is essential to reduce genomic instability during cell cycle progression²⁴. Spindle assembly and function are intimately associated with MT dynamics in a spatial and temporal manner during the cell cycle. Candidates coordinating spindle assembly and cell cycle regulation have been identified and implicated in carcinogenesis, including centrosomal factors such as pericentrin²⁵, noncentrosomal proteins such as nuclear mitotic apparatus protein (NuMA)²⁶, kinesin-like proteins, dynein/dynactin²⁷, and the small guanosine triphosphatase (GTPase) Ras-related nuclear protein Ran²⁸. TROAP, like the above-mentioned proteins, was validated as an MT-associated protein that maintains the structural and dynamic features of centrosomes, thereby contributing to normal spindle function. In this study, we found that TROAP depletion only had a mild nonsignificant increasing effect on the proportion of G₂/M phase cells by flow cytometry, whereas TROAP overexpression significantly rendered cells to accumulate in the G₁/S phase. In addition, correlation analysis also demonstrated that TROAP expression was associated with smaller tumor size and reduced nodule number in HCC. We therefore postulated that TROAP could delay cell cycle progression, thus inhibiting cellular proliferation and tumor growth in HCC through an MT-associated character. However, more data should be provided to demonstrate this point of view within the area of HCC.

Human embryo implantation is mediated by an array of adhesion molecules including L-selectin and trophinin²⁹. TROAP, as a cytoplasmic protein, forms a complex with trophinin intracellular domain to mediate the trophoblast-endometrial interaction and signaling transduction. After the initial attachment of embryonic cells to the maternal epithelial cells, a stronger adhesion is induced, and significant morphological changes are observed in the embryo implantation site. The cellular process of embryo implantation resembles those of malignant tumor cell metastasis and invasion, and they may share some molecular mechanisms with the trophoblast invasion of maternal uterine tissue^{14,15}. Our findings confirmed that TROAP downregulation enhanced cellular migration ability, while its overexpression caused an opposite effect in HCC cell models. Clinicopathological correlation analysis also revealed that the higher level of TROAP was correlated with mild vein invasion. These results suggested that TROAP may be involved in tumor metastasis. Crosstalk

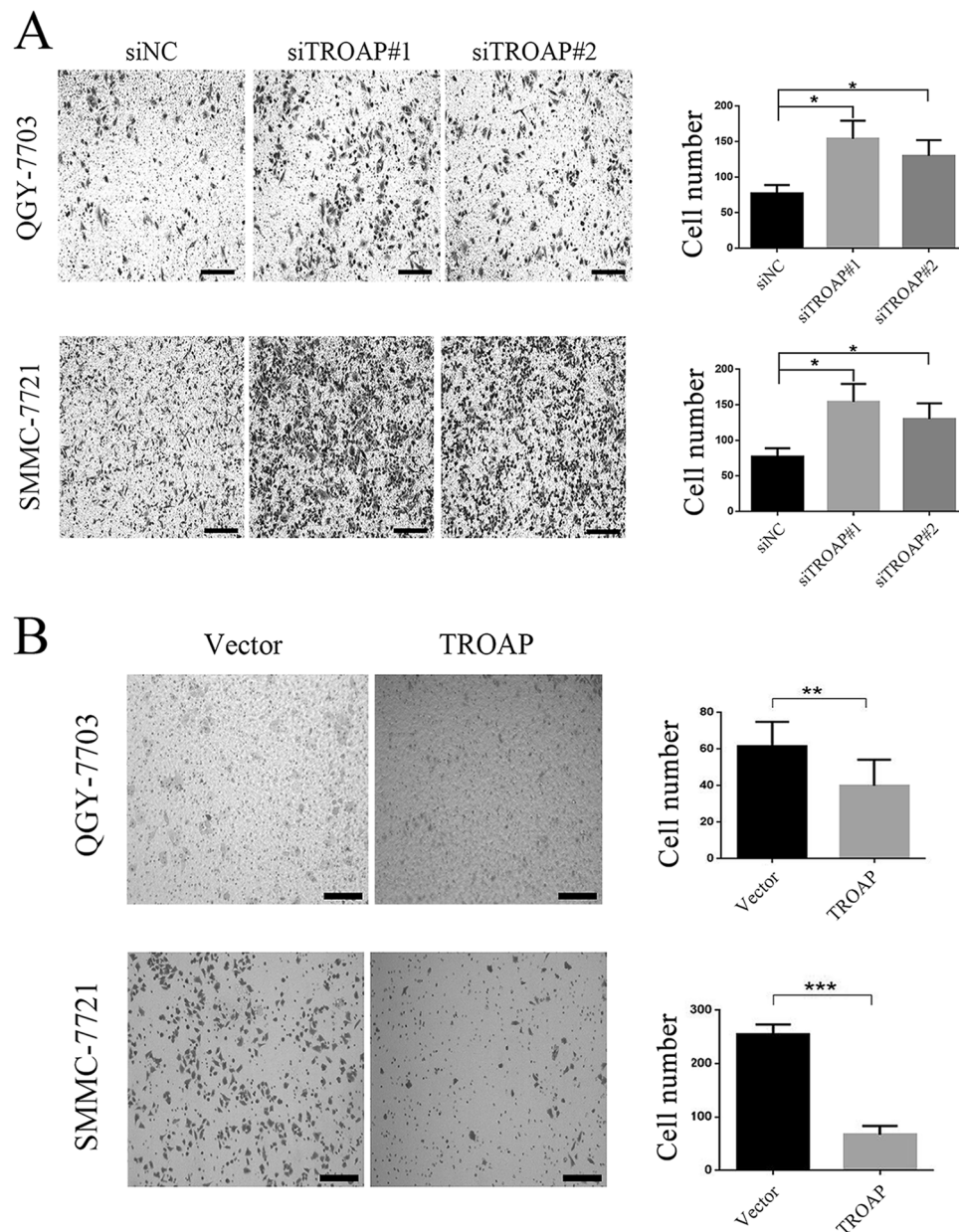


Figure 4. TROAP reduces the migration ability of HCC cells. (A) Transwell assay of QGY-7703 and SMMC-7721 cells transfected with control or TROAP siRNAs for 48 h. Left: representative images. Scale bars: 200 μ m. Right: quantification of average number of cells in the lower chamber per field. * p <0.05. (B) Transwell assay of control or TROAP-overexpressed QGY-7703 and SMMC-7721 cells. Left: representative images. Scale bars: 200 μ m. Right: quantification of average number of cells in lower chamber per field. ** p <0.01, *** p <0.001.

between the actin cytoskeleton and MTs promotes cellular migration, a process crucial for metastasis of cancer cells. Rho GTPase, such as RhoA, Ras-related C3 botulinum toxin substrate 1 (Rac1), and cell division cycle 42 (Cdc42) are among the major regulators that mediate the formation of different types of F-actin that confer changes in cortical tension and contraction³⁰. MTs extend to the cell periphery where localized factors cause changes in

their stability and dynamics, which influence the pathways that regulate F-actin polymerization, contributing to regulation of cellular migration¹¹. Previous studies have demonstrated that TROAP could be a microtubular cytoskeleton regulator with its ability to bind MT-based molecular motor T-complex-associated-testis-expressed 1 (Tctex-1)¹⁸. We proposed that TROAP may contribute to cancer cell metastasis by regulation of MT-associated

proteins. However, further investigations are also needed for demonstration.

To the best of our knowledge, this study is the first report that TROAP may directly participate in the regulation of cancer proliferation and metastasis in HCC. Through in vitro cell models, we provided evidence that high levels of TROAP could inhibit cellular growth, colony formation, and migration in HCC. TROAP expression in tumor tissue also significantly correlated with tumor size, nodule number, and vein invasion status in HCC. In summary, we proposed that TROAP may act as a potential diagnostic biomarker and therapeutic target for HCC.

ACKNOWLEDGMENTS: *This study was supported in part by grants from the National Natural Science Foundation of China (81371866), the International Cooperation Project of Guangzhou Science and Technology Program (2016201604030021), the National Grant Program on Key Infectious Disease (2014ZX10002002-002), and the major project of collaborative innovation of Guangzhou Science and Technology Program (201704020175). Author contributions: Yifan Lian: designed and performed experiments, generated figures, and drafted the manuscript; Weiming Fan: designed and performed experiments and generated figures; Hongbo Wang: analyzed the data; Yanlin Huang, Jialiang Wang, Liang Zhou, and Xiaojuan Wu: performed experiments; Meihai Deng: advice on the study design, collected samples and patient information, and ethical approval; Yuehua Huang: advised on the study design, supervised experiments and data analysis, critical review of manuscript, and provided funding. The authors declare no conflicts of interests.*

REFERENCES

1. Ferlay J, Soerjomataram I, Dikshit R, Eser S, Mathers C, Rebelo M, Parkin DM, Forman D, Bray F. Cancer incidence and mortality worldwide: Sources, methods and major patterns in GLOBOCAN 2012. *Int J Cancer* 2015; 136:E359–86.
2. Jemal A, Bray F, Center MM, Ferlay J, Ward E, Forman D. Global cancer statistics. *CA Cancer J Clin*. 2011;61:69–90.
3. Llovet JM, Zucman-Rossi J, Pikarsky E, Sangro B, Schwartz M, Sherman M, Gores G. Hepatocellular carcinoma. *Nat Rev Dis Primers* 2016;2:16018.
4. Zhu RX, Seto WK, Lai CL, Yuen MF. Epidemiology of hepatocellular carcinoma in the Asia-Pacific region. *Gut Liver* 2016;10:332–9.
5. El-Serag HB. Epidemiology of viral hepatitis and hepatocellular carcinoma. *Gastroenterology* 2012;142:1264–73. e1261.
6. Forner A, Gilabert M, Bruix J, Raoul JL. Treatment of intermediate-stage hepatocellular carcinoma. *Nat Rev Clin Oncol*. 2014;11:525–35.
7. Zucman-Rossi J, Villanueva A, Nault JC, Llovet JM. Genetic landscape and biomarkers of hepatocellular carcinoma. *Gastroenterology* 2015;149:1226–39. e1224.
8. Levvero M, Zucman-Rossi J. Mechanisms of HBV-induced hepatocellular carcinoma. *J Hepatol*. 2016;64:S84–101.
9. Sacristan C, Kops GJ. Joined at the hip: Kinetochores, microtubules, and spindle assembly checkpoint signaling. *Trends Cell Biol*. 2015;25:21–8.
10. Dominguez-Brauer C, Thu KL, Mason JM, Blaser H, Bray MR, Mak TW. Targeting mitosis in cancer: Emerging strategies. *Mol Cell* 2015;60:524–36.
11. Akhshi TK, Wernike D, Piekny A. Microtubules and actin crosstalk in cell migration and division. *Cytoskeleton (Hoboken)* 2014;71:1–23.
12. Fukuda MN, Sato T, Nakayama J, Klier G, Mikami M, Aoki D, Nozawa S. Trophinin and tascin, a novel cell adhesion molecule complex with potential involvement in embryo implantation. *Genes Dev*. 1995;9:1199–210.
13. Fukuda MN, Nozawa S. Trophinin, tascin, and bystin: A complex mediating unique attachment between trophoblastic and endometrial epithelial cells at their respective apical cell membranes. *Semin Reprod Endocrinol*. 1999;17:229–34.
14. Fukuda MN, Sugihara K, Nakayama J. Trophinin: What embryo implantation teaches us about human cancer. *Cancer Biol Ther*. 2008;7:1165.
15. Sugihara K, Sugiyama D, Byrne J, Wolf DP, Lowitz KP, Kobayashi Y, Kabir-Salmani M, Nadano D, Aoki D, Nozawa S, Nakayama J, Mustelin T, Ruoslahti E, Yamaguchi N, Fukuda MN. Trophoblast cell activation by trophinin ligation is implicated in human embryo implantation. *Proc Natl Acad Sci USA* 2007;104:3799–804.
16. Suzuki N, Nakayama J, Shih IM, Aoki D, Nozawa S, Fukuda MN. Expression of trophinin, tascin, and bystin by trophoblast and endometrial cells in human placenta. *Biol Reprod*. 1999;60:621–7.
17. Godoy H, Mhawech-Fauceglia P, Beck A, Miliotto A, Miller A, Lele S, Odunsi K. Developmentally restricted differentiation antigens are targets for immunotherapy in epithelial ovarian carcinoma. *Int J Gynecol Pathol*. 2013; 32:536–40.
18. Nadano D, Nakayama J, Matsuzawa S, Sato TA, Matsuda T, Fukuda MN. Human tascin, a proline-rich cytoplasmic protein, associates with the microtubular cytoskeleton. *Biochem J*. 2002;364:669–77.
19. Yang S, Liu X, Yin Y, Fukuda MN, Zhou J. Tascin is required for bipolar spindle assembly and centrosome integrity during mitosis. *FASEB J*. 2008;22:1960–72.
20. Dhanasekaran SM, Barrette TR, Ghosh D, Shah R, Varambally S, Kurachi K, Pienta KJ, Rubin MA, Chinnaiyan AM. Delineation of prognostic biomarkers in prostate cancer. *Nature* 2001;412:822–6.
21. Dhanasekaran R, Bandoh S, Roberts LR. Molecular pathogenesis of hepatocellular carcinoma and impact of therapeutic advances. *F1000Research* 2016;5:879
22. Goossens N, Sun X, Hoshida Y. Molecular classification of hepatocellular carcinoma: Potential therapeutic implications. *Hepat Oncol*. 2015;2:371–9.
23. Honda M, Yamashita T, Ueda T, Takatori H, Nishino R, Kaneko S. Different signaling pathways in the livers of patients with chronic hepatitis B or chronic hepatitis C. *Hepatology* 2006;44:1122–38.
24. Musacchio A, Salmon ED. The spindle-assembly checkpoint in space and time. *Nat Rev Mol Cell Biol*. 2007;8: 379–93.
25. Pihan GA, Purohit A, Wallace J, Knecht H, Woda B, Quesenberry P, Doxsey SJ. Centrosome defects and genetic instability in malignant tumors. *Cancer Res*. 1998; 58:3974–85.
26. Compton DA, Cleveland DW. NuMA is required for the proper completion of mitosis. *J Cell Biol*. 1993;120: 947–57.

27. Merdes A, Cleveland DW. Pathways of spindle pole formation: Different mechanisms; conserved components. *J Cell Biol.* 1997;138:953–56.
28. Ly TK, Wang J, Pereira R, Rojas KS, Peng X, Feng Q, Cerione RA, Wilson KF. Activation of the Ran GTPase is subject to growth factor regulation and can give rise to cellular transformation. *J Biol Chem.* 2010;285:5815–26.
29. Fukuda MN, Sugihara K. Cell adhesion molecules in human embryo implantation. *Sheng Li Xue Bao* 2012;64: 247–58.
30. Hall A. Rho family GTPases. *Biochem Soc Trans.* 2012; 40:1378–82.